

Search for Time-Dependent CPT Violation in Hadronic and Semileptonic B Decays

T. Higuchi,¹¹ K. Sumisawa,¹¹ I. Adachi,¹¹ H. Aihara,⁵⁴ D. M. Asner,⁴² V. Aulchenko,² T. Aushev,¹⁹
A. M. Bakich,⁴⁸ A. Bay,²⁶ K. Belous,¹⁷ V. Bhardwaj,³³ B. Bhuyan,¹³ M. Bischofberger,³³ A. Bondar,² A. Bozek,³⁷
M. Bračko,^{28,20} O. Brovchenko,²² T. E. Browder,¹⁰ M.-C. Chang,⁵ P. Chang,³⁶ A. Chen,³⁴ P. Chen,³⁶
B. G. Cheon,⁹ K. Chilikin,¹⁹ R. Chistov,¹⁹ I.-S. Cho,⁶⁰ K. Cho,²³ S.-K. Choi,⁸ Y. Choi,⁴⁷ J. Dalseno,^{29,50}
M. Danilov,¹⁹ Z. Doležal,³ Z. Drásal,³ S. Eidelman,² D. Epifanov,² J. E. Fast,⁴² V. Gaur,⁴⁹ N. Gabyshev,²
A. Garmash,² Y. M. Goh,⁹ B. Golob,^{27,20} J. Haba,¹¹ K. Hara,¹¹ K. Hayasaka,³² H. Hayashii,³³ Y. Horii,³²
Y. Hoshi,⁵² W.-S. Hou,³⁶ Y. B. Hsiung,³⁶ H. J. Hyun,²⁵ T. Iijima,^{32,31} K. Inami,³¹ A. Ishikawa,⁵³ R. Itoh,¹¹
Y. Iwasaki,¹¹ T. Iwashita,³³ T. Julius,³⁰ J. H. Kang,⁶⁰ P. Kapusta,³⁷ T. Kawasaki,³⁹ C. Kiesling,²⁹ H. J. Kim,²⁵
H. O. Kim,²⁵ J. B. Kim,²⁴ K. T. Kim,²⁴ M. J. Kim,²⁵ Y. J. Kim,²³ B. R. Ko,²⁴ S. Koblitz,²⁹ P. Kodyš,³
S. Korpar,^{28,20} P. Križan,^{27,20} P. Krokovny,² T. Kuhr,²² T. Kumita,⁵⁶ A. Kuzmin,² Y.-J. Kwon,⁶⁰ J. S. Lange,⁶
S.-H. Lee,²⁴ J. Li,⁴⁶ Y. Li,⁵⁸ J. Libby,¹⁴ C. Liu,⁴⁵ Z. Q. Liu,¹⁵ D. Liventsev,¹⁹ R. Louvot,²⁶ D. Matvienko,²
S. McOnie,⁴⁸ K. Miyabayashi,³³ H. Miyata,³⁹ Y. Miyazaki,³¹ G. B. Mohanty,⁴⁹ A. Moll,^{29,50} T. Mori,³¹
N. Muramatsu,⁴³ Y. Nagasaka,¹² Y. Nakahama,⁵⁴ M. Nakao,¹¹ H. Nakazawa,³⁴ Z. Natkaniec,³⁷ C. Ng,⁵⁴
S. Nishida,¹¹ K. Nishimura,¹⁰ O. Nitoh,⁵⁷ T. Nozaki,¹¹ S. Ogawa,⁵¹ T. Ohshima,³¹ S. Okuno,²¹ S. L. Olsen,^{46,10}
Y. Onuki,⁵⁴ P. Pakhlov,¹⁹ G. Pakhlova,¹⁹ C. W. Park,⁴⁷ H. K. Park,²⁵ K. S. Park,⁴⁷ R. Pestotnik,²⁰ M. Petrič,²⁰
L. E. Piilonen,⁵⁸ M. Prim,²² M. Ritter,²⁹ M. Röhrken,²² S. Ryu,⁴⁶ H. Sahoo,¹⁰ Y. Sakai,¹¹ T. Sanuki,⁵³
Y. Sato,⁵³ O. Schneider,²⁶ C. Schwanda,¹⁶ A. J. Schwartz,⁴ R. Seidl,⁴⁴ K. Senyo,⁵⁹ M. E. Sevir,³⁰ M. Shapkin,¹⁷
V. Shebalin,² C. P. Shen,³¹ T.-A. Shibata,⁵⁵ J.-G. Shiu,³⁶ B. Shwartz,² A. Sibidanov,⁴⁸ R. Sinha,¹⁸ P. Smerkol,²⁰
Y.-S. Sohn,⁶⁰ A. Sokolov,¹⁷ E. Solovieva,¹⁹ S. Stanič,⁴⁰ M. Starič,²⁰ M. Sumihama,⁷ T. Sumiyoshi,⁵⁶ S. Tanaka,¹¹
G. Tatishvili,⁴² Y. Teramoto,⁴¹ K. Trabelsi,¹¹ T. Tsuboyama,¹¹ M. Uchida,⁵⁵ S. Uehara,¹¹ T. Uglov,¹⁹ Y. Unno,⁹
S. Uno,¹¹ P. Urquijo,¹ Y. Usov,² G. Varner,¹⁰ K. E. Varvell,⁴⁸ A. Vinokurova,² V. Vorobyev,² C. H. Wang,³⁵
P. Wang,¹⁵ X. L. Wang,¹⁵ M. Watanabe,³⁹ Y. Watanabe,²¹ K. M. Williams,⁵⁸ E. Won,²⁴ B. D. Yabsley,⁴⁸
H. Yamamoto,⁵³ Y. Yamashita,³⁸ C. Z. Yuan,¹⁵ Y. Yusa,³⁹ Z. P. Zhang,⁴⁵ V. Zhilich,² and V. Zhulanov²

(The Belle Collaboration)

¹University of Bonn, Bonn

²Budker Institute of Nuclear Physics SB RAS and Novosibirsk State University, Novosibirsk 630090

³Faculty of Mathematics and Physics, Charles University, Prague

⁴University of Cincinnati, Cincinnati, Ohio 45221

⁵Department of Physics, Fu Jen Catholic University, Taipei

⁶Justus-Liebig-Universität Gießen, Gießen

⁷Gifu University, Gifu

⁸Gyeongsang National University, Chinju

⁹Hanyang University, Seoul

¹⁰University of Hawaii, Honolulu, Hawaii 96822

¹¹High Energy Accelerator Research Organization (KEK), Tsukuba

¹²Hiroshima Institute of Technology, Hiroshima

¹³Indian Institute of Technology Guwahati, Guwahati

¹⁴Indian Institute of Technology Madras, Madras

¹⁵Institute of High Energy Physics, Chinese Academy of Sciences, Beijing

¹⁶Institute of High Energy Physics, Vienna

¹⁷Institute of High Energy Physics, Protvino

¹⁸Institute of Mathematical Sciences, Chennai

¹⁹Institute for Theoretical and Experimental Physics, Moscow

²⁰J. Stefan Institute, Ljubljana

²¹Kanagawa University, Yokohama

²²Institut für Experimentelle Kernphysik, Karlsruher Institut für Technologie, Karlsruhe

²³Korea Institute of Science and Technology Information, Daejeon

²⁴Korea University, Seoul

²⁵Kyungpook National University, Taegu

²⁶École Polytechnique Fédérale de Lausanne (EPFL), Lausanne

²⁷Faculty of Mathematics and Physics, University of Ljubljana, Ljubljana

²⁸University of Maribor, Maribor

²⁹Max-Planck-Institut für Physik, München

³⁰University of Melbourne, School of Physics, Victoria 3010

³¹Graduate School of Science, Nagoya University, Nagoya

- ³²*Kobayashi-Maskawa Institute, Nagoya University, Nagoya*
³³*Nara Women's University, Nara*
³⁴*National Central University, Chung-li*
³⁵*National United University, Miao Li*
³⁶*Department of Physics, National Taiwan University, Taipei*
³⁷*H. Niewodniczanski Institute of Nuclear Physics, Krakow*
³⁸*Nippon Dental University, Niigata*
³⁹*Niigata University, Niigata*
⁴⁰*University of Nova Gorica, Nova Gorica*
⁴¹*Osaka City University, Osaka*
⁴²*Pacific Northwest National Laboratory, Richland, Washington 99352*
⁴³*Research Center for Nuclear Physics, Osaka University, Osaka*
⁴⁴*RIKEN BNL Research Center, Upton, New York 11973*
⁴⁵*University of Science and Technology of China, Hefei*
⁴⁶*Seoul National University, Seoul*
⁴⁷*Sungkyunkwan University, Suwon*
⁴⁸*School of Physics, University of Sydney, NSW 2006*
⁴⁹*Tata Institute of Fundamental Research, Mumbai*
⁵⁰*Excellence Cluster Universe, Technische Universität München, Garching*
⁵¹*Toho University, Funabashi*
⁵²*Tohoku Gakuin University, Tagajo*
⁵³*Tohoku University, Sendai*
⁵⁴*Department of Physics, University of Tokyo, Tokyo*
⁵⁵*Tokyo Institute of Technology, Tokyo*
⁵⁶*Tokyo Metropolitan University, Tokyo*
⁵⁷*Tokyo University of Agriculture and Technology, Tokyo*
⁵⁸*CNP, Virginia Polytechnic Institute and State University, Blacksburg, Virginia 24061*
⁵⁹*Yamagata University, Yamagata*
⁶⁰*Yonsei University, Seoul*

We report a new sensitive search for CPT violation, which includes improved measurements of the CPT -violating parameter z and the total decay-width difference normalized to the averaged width $\Delta\Gamma_d/\Gamma_d$ of the two B_d mass eigenstates. The results are based on a data sample of 535×10^6 $B\bar{B}$ pairs collected at the $\Upsilon(4S)$ resonance with the Belle detector at the KEKB asymmetric-energy e^+e^- collider. We obtain $\text{Re}(z) = [+1.9 \pm 3.7(\text{stat}) \pm 3.3(\text{syst})] \times 10^{-2}$, $\text{Im}(z) = [-5.7 \pm 3.3(\text{stat}) \pm 3.3(\text{syst})] \times 10^{-3}$, and $\Delta\Gamma_d/\Gamma_d = [-1.7 \pm 1.8(\text{stat}) \pm 1.1(\text{syst})] \times 10^{-2}$, all of which are consistent with zero. This is the most precise single measurement of these parameters in the neutral B -meson system to date.

PACS numbers: 14.40.Nd, 13.25.Hw, 11.30.Er

CPT invariance is one of the most fundamental theoretical concepts; its violation would have a serious impact on physics in general, and would require new physics beyond the Standard Model (SM). CPT violation requires the breakdown of some fundamental underlying physical assumption in the new physics beyond the SM, for example, violation of Lorentz invariance [1]. Several searches for CPT violation have been carried out; for example, the Belle and BaBar collaborations have published measurements of CPT -violating parameters in the neutral B -meson system [2-4], and the CPLEAR, KLOE, and KTeV collaborations have done so in the neutral K -meson system [5-7].

In the presence of CPT violation, the flavor and mass eigenstates of the neutral B mesons are related by $|B_L\rangle = p\sqrt{1-z}|B^0\rangle + q\sqrt{1+z}|\bar{B}^0\rangle$ and $|B_H\rangle = p\sqrt{1+z}|B^0\rangle - q\sqrt{1-z}|\bar{B}^0\rangle$, where $|B_L\rangle$ ($|B_H\rangle$) is a lighter (heavier) mass eigenstate. Here z is a complex parameter accounting for CPT violation; CPT is violated if $z \neq 0$. In the decay chain $\Upsilon(4S) \rightarrow B^0\bar{B}^0 \rightarrow f_{\text{rec}}f_{\text{tag}}$, where one of the B -mesons decays at time t_{rec} to a reconstructed final state f_{rec} and the other decays at time t_{tag} to a final state f_{tag} that distinguishes between B^0 and \bar{B}^0 , the most generic time-dependent decay rate with CPT violation allowed is given by [3]

$$\mathcal{P}(\Delta t; f_{\text{rec}} f_{\text{tag}}) = \frac{\Gamma_d}{2} e^{-\Gamma_d |\Delta t|} \left[\frac{|\eta_+|^2 + |\eta_-|^2}{2} \cosh\left(\frac{\Delta\Gamma_d}{2} \Delta t\right) - \mathcal{R}e(\eta_+^* \eta_-) \sinh\left(\frac{\Delta\Gamma_d}{2} \Delta t\right) + \frac{|\eta_+|^2 - |\eta_-|^2}{2} \cos(\Delta m_d \Delta t) + \mathcal{I}m(\eta_+^* \eta_-) \sin(\Delta m_d \Delta t) \right], \quad (1)$$

$$\eta_+ \equiv \mathcal{A}_{B^0 \rightarrow f_{\text{rec}}} \mathcal{A}_{\bar{B}^0 \rightarrow f_{\text{tag}}} - \mathcal{A}_{\bar{B}^0 \rightarrow f_{\text{rec}}} \mathcal{A}_{B^0 \rightarrow f_{\text{tag}}}, \quad (2)$$

$$\eta_- \equiv \sqrt{1 - z^2} \left(\frac{p}{q} \mathcal{A}_{B^0 \rightarrow f_{\text{rec}}} \mathcal{A}_{B^0 \rightarrow f_{\text{tag}}} - \frac{q}{p} \mathcal{A}_{\bar{B}^0 \rightarrow f_{\text{rec}}} \mathcal{A}_{\bar{B}^0 \rightarrow f_{\text{tag}}} \right) + z \left(\mathcal{A}_{B^0 \rightarrow f_{\text{rec}}} \mathcal{A}_{\bar{B}^0 \rightarrow f_{\text{tag}}} + \mathcal{A}_{\bar{B}^0 \rightarrow f_{\text{rec}}} \mathcal{A}_{B^0 \rightarrow f_{\text{tag}}} \right), \quad (3)$$

where $\Gamma_d \equiv (\Gamma_H + \Gamma_L)/2$, $\Delta\Gamma_d \equiv \Gamma_H - \Gamma_L$, $\Delta m_d \equiv m_H - m_L$, $\Delta t \equiv t_{\text{rec}} - t_{\text{tag}}$, and the $\mathcal{A}_{B^0, \bar{B}^0 \rightarrow f_{\text{rec}}, f_{\text{tag}}}$ are the relevant decay amplitudes. If f_{rec} is a CP eigenstate (f_{CP}), a parameter λ_{CP} , which characterizes CP violation, can be defined as $\lambda_{CP} \equiv (q/p)(\mathcal{A}_{\bar{B}^0 \rightarrow f_{CP}}/\mathcal{A}_{B^0 \rightarrow f_{CP}})$. The SM predicts $|\lambda_{CP}| \simeq 1$ and $\mathcal{I}m(\eta_{CP} \lambda_{CP}) \simeq \sin 2\phi_1$ for the case $f_{CP} = J/\psi K^0$, where η_{CP} is the CP eigenvalue of the final state.

In this paper we report improved results on the CPT -violating parameter z and normalized total-decay-width difference $\Delta\Gamma_d/\Gamma_d$ in $B^0 \rightarrow J/\psi K^0$ ($K^0 = K_S^0, K_L^0$), $B^0 \rightarrow D^{(*)-} h^+$ ($h^+ = \pi^+$ for D^- and π^+, ρ^+ for D^{*-}), and $B^0 \rightarrow D^{*-} \ell^+ \nu_\ell$ ($\ell^+ = e^+, \mu^+$) decays [8] using $535 \times 10^6 B\bar{B}$ pairs. Most of the sensitivity to $\mathcal{R}e(z)$ and $\Delta\Gamma_d/\Gamma_d$ is obtained from neutral B -meson decays to f_{CP} , while $\mathcal{I}m(z)$ is constrained primarily from other neutral B -meson decay modes.

The data sample is collected with the Belle detector at the KEKB asymmetric-energy e^+e^- collider [9] (3.5 on 8.0 GeV) operating at the $\Upsilon(4S)$ resonance. The $\Upsilon(4S)$ is produced with a Lorentz boost of $\beta\gamma = 0.425$ along the Z axis, which is antiparallel to the e^+ beam direction. Since $B\bar{B}$ pairs are produced approximately at rest in the $\Upsilon(4S)$ center-of-mass system (cms), Δt can be approximated from ΔZ , the difference between the Z coordinates of the two B decay vertices: $\Delta t \simeq \Delta Z/\beta\gamma c$.

The Belle detector [10] is a large-solid-angle magnetic spectrometer that consists of a silicon vertex detector (SVD), a 50-layer central drift chamber, an array of aerogel Cherenkov counters, a barrel-like arrangement of time-of-flight scintillation counters, an electromagnetic calorimeter comprised of CsI(Tl) crystals, located inside a superconducting solenoid coil that provides a 1.5 T magnetic field. An iron flux-return located outside of the coil is instrumented to detect K_L^0 mesons and to identify muons. Two inner detector configurations are used; a 2.0 cm radius beam pipe and a 3-layer SVD are used for the first data set (DS-I) of $152 \times 10^6 B\bar{B}$ pairs, while a 1.5 cm radius beam pipe, a 4-layer SVD, and a small-cell inner drift chamber are used to record the remaining data set (DS-II) of $383 \times 10^6 B\bar{B}$ pairs.

We reconstruct $B^0 \rightarrow f_{\text{rec}}$ decays in the $B^0 \rightarrow J/\psi K^0$, $D^- \pi^+$, $D^{*-} \pi^+$, $D^{*-} \rho^+$, and $D^{*-} \ell^+ \nu_\ell$ channels. We also reconstruct $B^+ \rightarrow J/\psi K^+$ and $\bar{D}^0 \pi^+$ to precisely determine parameters for the Δt -resolution function model in

neutral B decays. For the $J/\psi K_S^0$ and $J/\psi K_L^0$ modes, we use the same selection criteria as in Ref. [11]. Candidate $J/\psi K^+$ events are selected from combinations of a charged track and a J/ψ candidate using the same selection criteria as in $J/\psi K_S^0$. Charged and neutral charmed mesons are reconstructed in the $D^- \rightarrow K^+ \pi^- \pi^-$ and $\bar{D}^0 \rightarrow K^+ \pi^-, K^+ \pi^- \pi^0, K^+ \pi^- \pi^+ \pi^-$ decay modes, respectively. The invariant mass of their daughters, $M_{K\pi\pi}$, is required to be within $45 \text{ MeV}/c^2$ ($\sim 5\sigma$) of the nominal D -meson mass for the mode with π^0 , or $30 \text{ MeV}/c^2$ ($\sim 6\sigma$) for the other modes. Candidate D^{*-} mesons are reconstructed in $\bar{D}^0 \pi^-$ combinations, in which the mass difference M_{diff} between the D^{*-} and \bar{D}^0 candidates is required to be within $5 \text{ MeV}/c^2$ ($\sim 8\sigma$) of the nominal value. Candidate ρ^+ mesons are reconstructed from $\pi^+ \pi^0$ combinations with invariant mass within $225 \text{ MeV}/c^2$ of the nominal ρ^+ mass. For $D^{*-} \ell^+ \nu_\ell$ candidates the D^{*-} candidates are reconstructed using the D^{*-} and \bar{D}^0 decay modes listed above, where the detailed selection criteria are described in Ref. [12].

We identify B^0 or B^+ candidates in modes other than $B^0 \rightarrow J/\psi K_L^0$ or $D^{*-} \ell^+ \nu_\ell$ using the beam-energy constrained mass, $M_{\text{bc}} \equiv \sqrt{(E_{\text{beam}}^*)^2 - |\vec{p}_B^*|^2}$, and the energy difference, $\Delta E \equiv E_B^* - E_{\text{beam}}^*$, where E_{beam}^* is the beam energy in the cms, and E_B^* and \vec{p}_B^* are the cms energy and momentum of the reconstructed B candidate, respectively. The signal region is defined as $5.27 \text{ GeV}/c^2 \leq M_{\text{bc}} \leq 5.29 \text{ GeV}/c^2$ and a mode-dependent ΔE window within $|\Delta E| \lesssim 50 \text{ MeV}$. Candidate $B^0 \rightarrow J/\psi K_L^0$ decays are selected by requiring $0.20 \text{ GeV}/c \leq |\vec{p}_B^*| \leq 0.45 \text{ GeV}/c$. For $B^0 \rightarrow D^{*-} \ell^+ \nu_\ell$ decays, the energies and momenta of the B meson and $D^* \ell$ system in the cms satisfy $M_{\nu_\ell}^2 = (E_B^* - E_{D^* \ell})^2 - (|\vec{p}_B^*|^2 + |\vec{p}_{D^* \ell}^*|^2 - 2|\vec{p}_B^*||\vec{p}_{D^* \ell}^*| \cos \theta_{B, D^* \ell})$, where M_{ν_ℓ} is the neutrino mass and $\cos \theta_{B, D^* \ell}$ is the angle between \vec{p}_B^* and $\vec{p}_{D^* \ell}^*$. We calculate $\cos \theta_{B, D^* \ell}$ setting $M_{\nu_\ell} = 0$ and $E_B^* = E_{\text{beam}}^*$. The signal region is defined as $|\cos \theta_{B, D^* \ell}| < 1.1$. In the $\cos \theta_{B, D^* \ell}$ signal region, $B^0 \rightarrow D^{*-} \ell^+ \nu_\ell$ decays are also reconstructed. Since the Δt distribution is expected to be the same as that in $D^{*-} \ell^+ \nu_\ell$, we treat $B^0 \rightarrow D^{*-} \ell^+ \nu_\ell$ decays as signal.

The event-by-event signal probability is estimated from signal and background distributions of the kinematic parameters, M_{bc} , ΔE , \vec{p}_B^* , and $\cos \theta_{B, D^* \ell}$. Signal and combinatorial background distributions in M_{bc}

are modeled by Gaussians and an empirically determined background shape with a kinematic threshold originally introduced by ARGUS [13], respectively, while those in ΔE are modeled by the sum of two Gaussians and a first-order polynomial, respectively. The event-by-event signal probability parameters for the $D^{(*)-}h^+$ modes are determined from signal and sideband M_{bc} distributions with an additional background component from B decays that peaks in M_{bc} (peaking background), which is modeled by an ad-hoc distribution estimated from Monte Carlo (MC) simulation. For the $J/\psi K_S^0$ and $J/\psi K^+$ modes, we perform a two-dimensional fit to the M_{bc} - ΔE distributions, neglecting the small contribution from the peaking background. The signal and most of the background distributions in \vec{p}_B^* and $\cos\theta_{B,D^*\ell}$ for the $J/\psi K_L^0$ and $D^{*-}\ell^+\nu_\ell$ modes are modeled using MC simulation, while the background contribution from incorrectly reconstructed J/ψ mesons in $J/\psi K_L^0$ and incorrectly reconstructed D^{*-} mesons in $D^{*-}\ell^+\nu_\ell$ are modeled using sideband regions of the J/ψ and D^{*-} , respectively.

The b -flavor of f_{tag} is identified from inclusive properties of particles that are not associated with the $B^0, \bar{B}^0 \rightarrow f_{\text{rec}}$ decay. The tagging information is represented by two event-by-event parameters, the b -flavor charge q_{tag} and a MC-determined flavor-tagging dilution factor r [14]. The parameter r ranges from $r = 0$ for no flavor discrimination to $r = 1$ for unambiguous flavor assignment. For events with $r > 0.1$, the wrong tag fractions for six r intervals, w_l ($l = 1 \dots 6$), and their differences between B^0 and \bar{B}^0 decays, Δw_l , are determined using the data sample as described later. If $r \leq 0.1$, we set the wrong tag fraction to 0.5 so that the event is not used on flavor tagging.

The vertex position is reconstructed using charged tracks that have sufficient SVD hits [15]. The f_{rec} vertex for the modes with a J/ψ is reconstructed using lepton tracks from the J/ψ decay, while in modes without a J/ψ the f_{rec} vertex is reconstructed by combining the \bar{D}^0 - or D^- -meson trajectory and the remaining charged track; the slow π^- from the D^{*-} decay is not included because of its poor position resolution. The f_{tag} vertex is obtained from selected well-reconstructed tracks that are not assigned to f_{rec} . A constraint on the interaction region profile (IP) in the plane perpendicular to the Z axis is also applied to both f_{rec} and f_{tag} reconstructed vertices. We model the Δt -resolution function as a convolution of four sub-components [15]: detector resolutions for f_{rec} and f_{tag} vertex reconstruction, boost effect due to non-primary particle decays in f_{tag} , and dilution by the kinematic approximation $\Delta t \simeq \Delta Z/(\beta\gamma)c$. Nearly all model parameters are determined using the data as described later. The exceptions are the parameters for the boost effect and kinematic approximation, which are obtained using MC simulation. For candidate events in which both B vertices are found, for further analysis, we only use events with vertices that satisfy $|\Delta t| < 70$ ps and $\xi_{\text{rec}}, \xi_{\text{asc}} < 250$, where ξ is the χ^2 of the vertex fit calculated only along the Z direction [12].

TABLE I: Number of events N_{ev} and purity in the signal region for each decay mode.

B decay mode	N_{ev}	Purity (%)
$J/\psi K_S^0$	7713	97.0
$J/\psi K_L^0$	10966	59.2
$D^- \pi^+$	39366	83.2
$D^{*-} \pi^+$	46292	81.5
$D^{*-} \rho^+$	45913	66.3
$D^{*-} \ell^+ \nu_\ell$	383818	75.2
$J/\psi K^+$	32150	97.3
$\bar{D}^0 \pi^+$	216605	63.9

After flavor tagging and vertex reconstruction, we count the number of events remaining in the signal region N_{ev} and estimate the purity for each decay mode. The values of N_{ev} and purities for each mode are listed in Table I.

We determine three major physics parameters $\mathcal{R}e(z)$, $\mathcal{I}m(z)$, and $\Delta\Gamma_d/\Gamma_d$ together with five other physics parameters τ_{B^0}, τ_{B^+} (neutral and charged B -meson lifetimes), Δm_d , $|\lambda_{CP}|$, and $\arg(\eta_{CP}\lambda_{CP})$ in a simultaneous 72-parameter fit to the observed Δt distribution. The remaining 64 parameters are the Δt -resolution function model parameters (34), flavor-tagging parameters w_l and Δw_l (24), and background parameters for $B^0 \rightarrow D^{*-}\ell^+\nu_\ell$ (6). The non-physics parameters are determined separately for DS-I and DS-II. An unbinned fit is performed by maximizing a likelihood function defined by $L(\mathcal{R}e(z), \mathcal{I}m(z), \Delta\Gamma_d/\Gamma_d) = \prod_i P^i(\mathcal{R}e(z), \mathcal{I}m(z), \Delta\Gamma_d/\Gamma_d; \Delta t^i, q_{\text{tag}}^i)$, where the product is over all events in the signal region. The likelihood P^i for the i -th event is given by

$$P^i = (1 - f_{\text{ol}}) f_{\text{sig}}^i \mathcal{P}(\Delta t^i; f_{\text{rec}}^i, f_{\text{tag}}^i) \otimes R^i(\Delta t^i) + (1 - f_{\text{ol}}) \sum_k f_{\text{bkg}}^{k,i} P_{\text{bkg}}^k(\Delta t^i) + f_{\text{ol}} P_{\text{ol}}(\Delta t^i). \quad (4)$$

The first term accounts for the signal component, where f_{sig}^i is an event-by-event signal fraction. In Eq. (4) \mathcal{P} is modified from Eq. (1) by including the event-by-event incorrect-tagging effect, w_l^i and Δw_l^i , and the symbol \otimes indicates a convolution with the Δt -resolution function $R^i(\Delta t)$. The second term accounts for the background component, where $f_{\text{bkg}}^{k,i}$ is an event-by-event background fraction and k runs over all background categories. The signal and background fractions are normalized to $f_{\text{sig}}^i + \sum_k f_{\text{bkg}}^{k,i} = 1$. The Δt -distribution for the combinatorial background component is modeled using the sideband region of ΔE - M_{bc} , \vec{p}_B^* , or $\cos\theta_{B,D^*\ell}$ space, while the Δt distribution for the peaking-background components are modeled by MC. The third term accounts for a small but broad (Δt outlier) component that cannot be described by the first and second terms, where f_{ol} is an event-dependent outlier fraction and $P_{\text{ol}}(\Delta t)$ is a broad Gaussian. In the nominal fit, we account for

CKM-favored $B \rightarrow \bar{D}$ decay via $b \rightarrow \bar{c}ud$ (CFD) but neglect the contribution from CKM-suppressed $B \rightarrow D$ decay via $b \rightarrow \bar{u}cd$ (CSD) both in f_{rec} and f_{tag} . The effect of the CSD is included in the systematic uncertainty.

From the fit to the data, we obtain $\mathcal{R}e(z) = (+1.9 \pm 3.7) \times 10^{-2}$, $\mathcal{I}m(z) = (-5.7 \pm 3.3) \times 10^{-3}$, and $\Delta\Gamma_d/\Gamma_d = (-1.7 \pm 1.8) \times 10^{-2}$, together with $\tau_{B^0} = 1.531 \pm 0.004$ ps, $\tau_{B^+} = 1.640 \pm 0.006$ ps, $\Delta m_d = 0.506 \pm 0.003$ ps $^{-1}$, $|\lambda_{CP}| - 1 = (1.1 \pm 3.8) \times 10^{-3}$, and $\arg(\eta_{CP}\lambda_{CP}) = -0.700 \pm 0.042$, where all uncertainties are statistical only. The fit has a two-fold ambiguity in the sign of $\mathcal{R}e(\eta_{CP}\lambda_{CP})$; $\mathcal{R}e(z)$ and $\Delta\Gamma_d/\Gamma_d$ change signs depending on its sign. We take the solution with positive $\mathcal{R}e(\eta_{CP}\lambda_{CP})$, which is the result of the global fit [17]. The correlation coefficients ρ between two of the three major physics parameters are $\rho_{\mathcal{R}e(z), \mathcal{I}m(z)} = -0.17$, $\rho_{\mathcal{R}e(z), \Delta\Gamma_d/\Gamma_d} = +0.08$, and $\rho_{\mathcal{I}m(z), \Delta\Gamma_d/\Gamma_d} = +0.09$. The largest correlation coefficient between a major physics parameter and any other fit parameter is $\rho_{\mathcal{R}e(z), \Delta m_d} = +0.24$. The fitted values of $|\lambda_{CP}|$ and $\arg(\eta_{CP}\lambda_{CP})$ give $\sin 2\phi_1 = 0.645 \pm 0.032(\text{stat})$, which is consistent with our dedicated $\sin 2\phi_1$ measurement with the same data sample [11], because the major physics parameters are consistent with zero. Figures 1 and 2 show the Δt distributions for events with $f_{\text{rec}} = J/\psi K^0$ cases and the other cases, respectively, with the fitted curves superimposed.

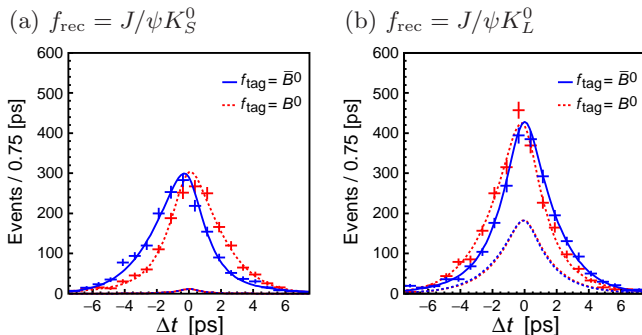


FIG. 1: Δt distributions for events with flavor tag quality $r > 0.5$, where (a) and (b) corresponds to $f_{\text{rec}} = J/\psi K_S^0$ and $J/\psi K_L^0$ cases, respectively. Events are separated according to tagged f_{tag} flavor, where the solid and dashed curves are for $q_{\text{tag}} = +1$ and -1 events, respectively. The two dashed curves below the fit curves indicate the sum of the background and outlier components for each f_{tag} flavor, which are almost indistinguishable because of their similar shapes.

To illustrate the CPT sensitivity of our measurements, we plot the deviations of the asymmetries from the fit with $\mathcal{R}e(z) = \mathcal{I}m(z) = \Delta\Gamma_d/\Gamma_d = 0$ in Figure 3, where (a), (b), and (c) show those for CP asymmetries of $B^0 \rightarrow J/\psi K_S^0$, $J/\psi K_L^0$, and opposite-flavor B -meson pairs, respectively; (d) shows asymmetries between the opposite-flavor and same-flavor B -meson pairs. Asymmetries are obtained from events in Δt bins without background subtraction, where the events are required to have $r > 0.5$. We superimpose the nominal fit curves and those

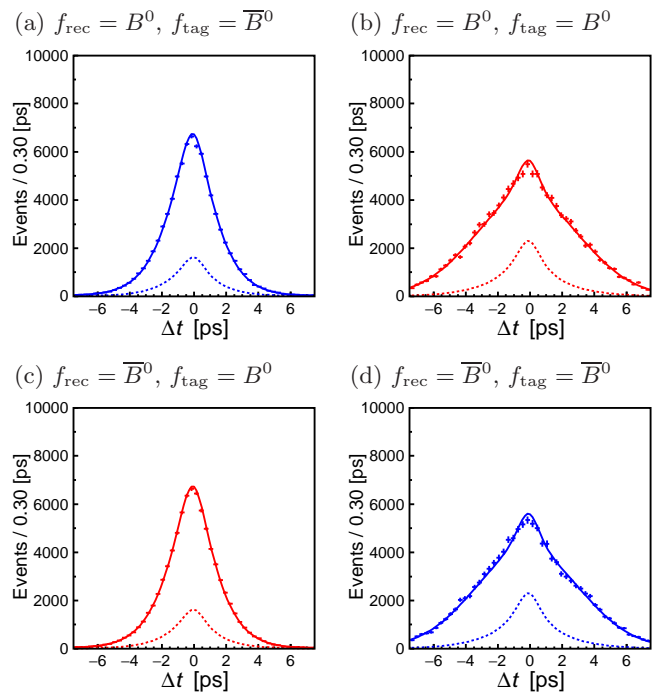


FIG. 2: Δt distributions for events with flavor tag quality $r > 0.5$, where (a, b) and (c, d) corresponds to flavor-specific $f_{\text{rec}} = B^0$ and \bar{B}^0 cases, respectively. The dashed curve below the fit curve indicates the sum of the background and outlier components.

TABLE II: Summary of systematic uncertainties on the major physics parameters.

Source	$\delta(\mathcal{R}e(z))$	$\delta(\mathcal{I}m(z))$	$\delta(\Delta\Gamma_d/\Gamma_d)$
Vertex reconstruction	0.008	0.0028	0.009
Δt -resolution function	0.003	0.0004	0.002
Tag-side interference	0.028	0.0006	0.001
CSD effect	0.004	0.0008	0.003
Fit bias	0.012	0.0013	0.005
Signal fraction	0.004	0.0002	0.002
Background Δt shape	0.005	0.0001	0.002
Others	0.001	< 0.0001	0.002
Total	0.033	0.0033	0.011

with one parameter shifted by $\sim 5\sigma$ in each subsample fit. For illustration, the most appropriate parameter is chosen in each plot.

Table II lists the systematic uncertainties on the major physics parameters. The total systematic uncertainty is obtained by adding the contributions in Table II in quadrature. The dominant contributions are from the tag-side interference (TSI) [16] and vertex reconstruction; the next largest contributions are from fit bias.

The TSI effect arises from the interference between CFD and CSD amplitudes in f_{tag} . In general, the pres-

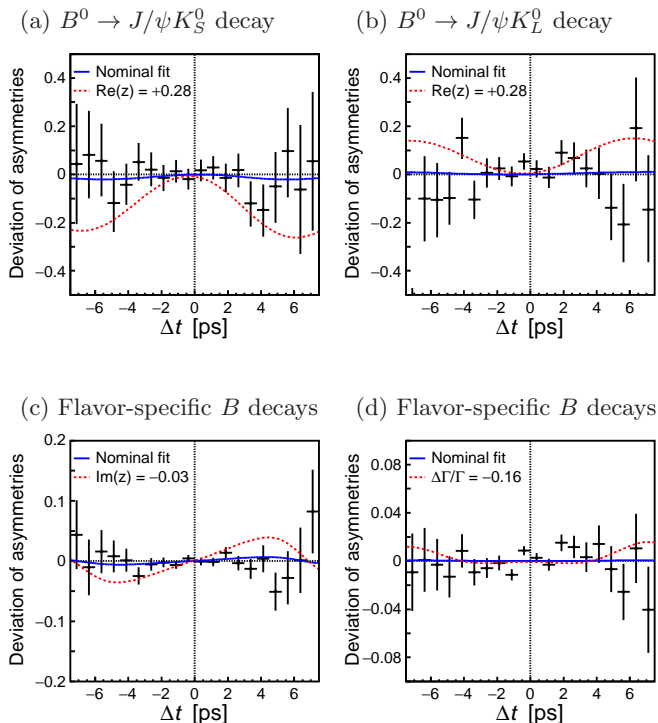


FIG. 3: Deviations of the asymmetries from the fit with $\mathcal{R}e(z) = \mathcal{I}m(z) = \Delta\Gamma_d/\Gamma_d = 0$. The crosses with error bars are data. The solid curves are nominal fits. The dashed curves are with $\mathcal{R}e(z) = +0.28$ for (a) and (b), $\mathcal{I}m(z) = -0.03$ for (c), and $\Delta\Gamma_d/\Gamma_d = -0.16$ for (d) (see text for details).

ence of CSD introduces new terms in Eqs. (2) and (3)

$$\begin{aligned} \mathcal{A}_{B^0 \rightarrow f_{\text{CSD}}} &= R_f \exp[i(+\phi_3 + \delta_f)], \\ \mathcal{A}_{\bar{B}^0 \rightarrow f_{\text{CSD}}} &= R_f \exp[i(-\phi_3 + \delta_f)], \end{aligned} \quad (5)$$

where R_f and δ_f are the mode-dependent ratio of the CSD to CFD amplitudes and the relative strong-phase difference between the CSD and CFD amplitudes, respectively, and $\phi_3 = 67.2^\circ$ [17]. For the tag-side parameter, $R_{f_{\text{tag}}}$ and $\delta_{f_{\text{tag}}}$ are “effective” values because f_{tag} is an admixture of several decay modes, some of which do not have a corresponding CSD. The effective $R_{f_{\text{tag}}}$ and $\delta_{f_{\text{tag}}}$ parameters are estimated using the $B^0 \rightarrow D^{*\mp} \ell^+ \nu_\ell$ sample [12]. We perform fits to the major physics parameters varying the terms from Eqs. (5) into Eqs. (2) and (3). The deviation from the nominal fit is quoted as a systematic uncertainty.

The CSD effects in f_{rec} are investigated by performing fits of the major physics parameters varying the R_f and δ_f parameters introduced in Eqs. (5). For the $D^- \pi^+$ and $D^{*-} \pi^+$ modes, we use $R_{D\pi} = 0.02$ or $R_{D^* \pi} = 0.02$ predicted in Ref. [18], and $\delta_{D^{(*)}h}$ computed from measurements of CP -violating parameters in the relevant B decays [19]. We quote fitted deviations as the systematic uncertainties. For the $D^{*-} \rho^+$ mode, we assume $R_{D\rho} = 0.02$, and allow $\delta_{D^* \rho}$ to be 0° , 90° , 180° , or 270° , because of the absence of CP -violating parameter mea-

surements. We quote the largest fitted deviation as the systematic uncertainty.

The systematic uncertainty due to vertex reconstruction is estimated as follows. We repeat fits by changing various requirements or parameters used in the vertex reconstruction: the IP constraint, the track selection criteria, and the calibration of the track position and momentum uncertainties. The deviation from the nominal fit is quoted as the systematic uncertainty. Systematic errors due to imperfect SVD alignment are estimated from MC samples with artificially varied alignment constants. Effects from small biases in the ΔZ measurement observed in $e^+e^- \rightarrow \mu^+\mu^-$ and other control samples are accounted for by applying a special correction function and including the variation from the nominal result into the systematic uncertainty.

We estimate the fit biases $\delta_{\mathcal{R}e(z)}^{\text{bias}}$, $\delta_{\mathcal{I}m(z)}^{\text{bias}}$, and $\delta_{\Delta\Gamma_d/\Gamma_d}^{\text{bias}}$ using an analysis procedure with signal MC simulation. We generate sets of Δt distributions with statistics similar to data, fixing $(\mathcal{R}e(z), \mathcal{I}m(z), \Delta\Gamma_d/\Gamma_d) = (0, 0, 0)$ or varying one of the three input parameters to $\mathcal{R}e(z) = \pm 0.01$, $\mathcal{I}m(z) = \pm 0.01$, or $\Delta\Gamma_d/\Gamma_d = \pm 0.05$. We perform a full-parameter fit to each generated distribution without the background component, and take deviations of the fitted three parameters from the input value as the bias. We quote the average value of biases in the above seven samples. These effects are included into the systematic uncertainty after symmetrization.

The systematic uncertainty due to the Δt -resolution function is estimated by varying by $\pm 2\sigma$ each resolution-function parameter determined from MC, and repeating the fit to add each variation in quadrature. We also take the systematic effect from the Δt -outlier elimination criteria into account in the systematic uncertainty by varying each criterion and adding each variation in quadrature.

The most precise previous results on the CPT -violating parameter and $\Delta\Gamma_d/\Gamma_d$ in the neutral B -meson system were obtained by the BaBar collaboration. They found $\mathcal{R}e(\lambda_{CP}/|\lambda_{CP}|)\mathcal{R}e(z) = +0.014 \pm 0.035(\text{stat}) \pm 0.034(\text{syst})$, $\mathcal{I}m(z) = (-13.9 \pm 7.3(\text{stat}) \pm 3.3(\text{syst})) \times 10^{-3}$, and $\text{sgn}(\mathcal{R}e(\lambda_{CP}))\Delta\Gamma_d/\Gamma_d = -0.008 \pm 0.037(\text{stat}) \pm 0.018(\text{syst})$ [3,4]. For $\mathcal{R}e(\lambda_{CP}/|\lambda_{CP}|)\mathcal{R}e(z)$, our result is $(+1.5 \pm 3.8) \times 10^{-2}$, where the total error is quoted. Our result is consistent with Ref. [4] and improves the overall precision by factors of 1.3 to 2.0 for all parameters.

In summary, we report a new search for CPT violation with an improved measurement of the CPT -violating parameter z and normalized decay-rate difference $\Delta\Gamma_d/\Gamma_d$ in $B^0 \rightarrow J/\psi K_S^0$, $J/\psi K_L^0$, $D^- \pi^+$, $D^{*-} \pi^+$, $D^{*-} \rho^+$, and $D^{*-} \ell^+ \nu_\ell$ decays using $535 \times 10^6 B\bar{B}$ pairs collected at the $\Upsilon(4S)$ resonance with the Belle detector. We find

$$\begin{aligned} \mathcal{R}e(z) &= [+1.9 \pm 3.7(\text{stat}) \pm 3.3(\text{syst})] \times 10^{-2}, \\ \mathcal{I}m(z) &= [-5.7 \pm 3.3(\text{stat}) \pm 3.3(\text{syst})] \times 10^{-3}, \text{ and} \\ \Delta\Gamma_d/\Gamma_d &= [-1.7 \pm 1.8(\text{stat}) \pm 1.1(\text{syst})] \times 10^{-2}, \end{aligned}$$

all of which are consistent with zero. This is the most precise measurement of CPT -violating parameters in the neutral B -meson system to date.

We thank the KEKB group for excellent operation of the accelerator; the KEK cryogenics group for efficient solenoid operations; and the KEK computer group, the NII, and PNNL/EMSL for valuable computing and SINET4 network support. We acknowledge support from

MEXT, JSPS and Nagoya's TLPRC (Japan); ARC and DIISR (Australia); NSFC (China); MSMT (Czechia); DST (India); INFN (Italy); MEST, NRF, GSDC of KISTI, and WCU (Korea); MNiSW (Poland); MES and RFAAE (Russia); ARRS (Slovenia); SNSF (Switzerland); NSC and MOE (Taiwan); and DOE and NSF (USA).

-
- [1] O. W. Greenberg, Phys. Rev. Lett. **89**, 231602 (2002); V. A. Kostelecký, Phys. Rev. D **69**, 105009 (2004).
- [2] N. Hastings *et al.* (Belle Collaboration), Phys. Rev. D **67**, 052004 (2003).
- [3] B. Aubert *et al.* (BaBar Collaboration), Phys. Rev. D **70**, 012007 (2004); B. Aubert *et al.* (BaBar Collaboration), Phys. Rev. Lett. **92**, 181801 (2004).
- [4] B. Aubert *et al.* (BaBar Collaboration), Phys. Rev. Lett. **96**, 251802 (2006).
- [5] A. Angelopoulos *et al.* (CLEAR Collaboration), Eur. Phys. J. C **22**, 55 (2001).
- [6] F. Ambrosino *et al.* (KLOE Collaboration), JHEP **0612**, 011 (2006).
- [7] E. Abouzaid *et al.* (KTeV Collaboration), Phys. Rev. D **83**, 092001 (2011).
- [8] Throughout this paper, the inclusion of the charge-conjugate decay modes is implied unless otherwise stated.
- [9] S. Kurokawa and E. Kikutani, Nucl. Instrum. Methods Phys. Res., Sect. A **499**, 1 (2003), and other papers included in this volume.
- [10] A. Abashian *et al.* (Belle Collaboration), Nucl. Instrum. Methods Phys. Res., Sect. A **479**, 117 (2002).
- [11] K.-F. Chen *et al.* (Belle Collaboration), Phys. Rev. Lett. **98**, 031802 (2007).
- [12] K. Abe *et al.* (Belle Collaboration), Phys. Rev. D **71**, 072003 (2005).
- [13] H. Albrecht *et al.* (ARGUS Collaboration), Phys. Lett. B **241**, 278 (1990).
- [14] H. Kakuno *et al.*, Nucl. Instrum. Methods Phys. Res., Sect. A **533**, 516 (2004).
- [15] H. Tajima *et al.*, Nucl. Instrum. Methods Phys. Res., Sect. A **533**, 370 (2004).
- [16] O. Long, M. Baak, R. N. Cahn, and D. Kirkby, Phys. Rev. D **68**, 034010 (2003).
- [17] J. Charles *et al.* (CKMfitter Group), Eur. Phys. J. C **41**, 1 (2005), results at ICHEP2010 at <http://ckmfitter.in2p3.fr>
- [18] D. A. Suprun, C.-W. Chiang, and J. L. Rosner, Phys. Rev. D **65**, 054025 (2002).
- [19] S. Bahinipati *et al.* (Belle Collaboration), Phys. Rev. D **84**, 021101(R) (2011); B. Aubert *et al.* (BaBar Collaboration), Phys. Rev. D **73**, 111101(R) (2006); F. J. Ronga *et al.* (Belle Collaboration), Phys. Rev. D **73**, 092003 (2006); B. Aubert *et al.* (BaBar Collaboration), Phys. Rev. D **71**, 112003 (2005).